processes

MDPI

Article

Physical Properties of Moist, Fermented Corn Kernels

Keagan J. Blazer [1], Kevin J. Shinners [1,*], Zachary A. Kluge [1], Mehari Z. Tekeste [2] and Matthew F. Digman [1]

[1] Department of Biological Systems Engineering, University of Wisconsin, Madison, WI 53706, USA
[2] Department of Agricultural and Biosystems Engineering, Iowa State University, Ames, IA 50011, USA
* Correspondence: kevin.shinners@wisc.edu (K.J.S.); Tel.: +1-608-262-3310

Abstract: A novel approach to producing corn stover biomass feedstock has been investigated. In this approach, corn grain and stover are co-harvested at moisture contents much less than typical corn silage. The grain and stover are conserved together by anaerobic storage and fermentation and then separated before end use. When separated from the stover, the moist, fermented grain had physical characteristics that differ from typical low-moisture, unfermented grain. A comprehensive study was conducted to quantify the physical properties of this moist, fermented grain. Six corn kernel treatments, either fermented or unfermented, having different moisture contents, were used. Moist, fermented kernels (26 and 36% w.b. moisture content) increased in size during storage. The fermented kernels' widths and thicknesses were 10% and 15% greater, respectively, and their volume was 28% greater than the dry kernels (15% w.b.). Dry basis particle density was 9% less for moist, fermented kernels. Additionally, the dry basis bulk density was 29% less, and the dry basis hopper-discharged mass flow rate was 36% less. Moist, fermented grain had significantly greater kernel-to-kernel coefficients of friction and angles of repose compared to relatively dry grain. The friction coefficient on four different surfaces was also significantly greater for fermented kernels. Fermented corn kernels had lower individual kernel rupture strengths than unfermented kernels. These physical differences must be considered when designing material handling and processing systems for moist, fermented corn grain.

Keywords: corn; density; fermented; flow; friction; kernels; properties; repose

Citation: Blazer, K.J.; Shinners, K.J.; Kluge, Z.A.; Tekeste, M.Z.; Digman, M.F. Physical Properties of Moist, Fermented Corn Kernels. *Processes* **2023**, *11*, 1351. https://doi.org/10.3390/pr11051351

Academic Editors: Pavel Mokrejš and Chi-Fai Chau

Received: 23 March 2023
Revised: 22 April 2023
Accepted: 24 April 2023
Published: 27 April 2023

1. Introduction

Both corn grain and the non-grain portion of the plant (corn stover) can be valuable feedstocks for bio-energy and bio-products' production. Corn grain and stover are typically harvested in separate field operations with a different suite of machines. The typical bale-based system of harvesting corn stover has many negative issues and is not economical [1]. An alternative approach to corn grain and stover harvest has been investigated that involves the co-harvest with a single machine, anerobic co-storage, and co-transport of these two components, followed by grain and stover separation at a biorefinery [2,3]. While harvest is proposed to occur at typical grain moisture of less than 25% (w.b.), the stover moisture would typically be 30% to 55% (w.b.) [4]. Successful conservation of the co-stored fractions of corn grain and stover is facilitated by anerobic storage and fermentation of both fractions. In the final steps of this novel system, the grain and stover would be co-transported to a biorefinery where the two fractions would be separated to accommodate the different end uses for starch and cellulose. The stover fraction could be used as a biofuel or bioproduct feedstock. The corn grain could be used for conversion to ethanol, for instance, or could be used for animal feed.

During prolonged anerobic storage, the corn kernels gain moisture from the moist stover [4]. A system employing a combination of air classification and mechanical sieving has been developed, in which up to 97% of the moist, fermented grain was separated from the stover [5]. Due to the gain in moisture during storage and subsequent fermentation,

the separated grain may have very different physical properties than typical dry corn grain used at most biorefineries. In this new system, knowledge of the physical properties of fermented corn grain is essential for designing material handling, storage, and processing technologies. Physical properties are helpful in establishing grain flow characteristics, understanding potential for grain damage from handling, and suggesting appropriate processing equipment. Information on physical properties exists for low moisture corn grain (i.e., < 25% w.b.) [6,7], but there is virtually no published information on the physical properties of fermented corn kernels above the 25% w.b. moisture range.

Moisture content has a strong impact on unfermented corn kernel physical properties. Within the range of moisture from 5% to 22%, corn kernels tended to expand when rewetted, and the kernel friction coefficient on various surfaces increased [8]. Each principal dimension linearly increased dependent on the moisture content within the range of 5–19% (w.b.) [9]. An increase in kernel size and shape with moisture content resulted in decreased bulk density and increased porosity [7–10]. The angle of repose increased with kernel surface roughness, friction coefficient, and moisture content [11,12]. Mass flow rate decreased by 20% when corn kernel moisture increased from 16% to 26% (w.b.) [7]. The corn kernel rupture force decreased as the kernel moisture increased from 13% to 29% (w.b.) [13]. Increasing moisture content from 10–26% (w.b.) changed the mechanical behavior of corn kernels from brittle to viscoelastic [10]. The angle of internal friction and apparent cohesion increased as the kernel moisture content increased from 11% to 26% (w.b.) [7]. Although none of these studies were conducted with fermented corn kernels or at the level of moisture content used in this research, it is clear that kernel moisture content has a strong influence on the physical–mechanical properties of corn kernels.

The corn kernel properties changed during anerobic storage with moist corn stover. Pike et al. [4] reported that moisture migrated from the moist stover to the drier grain during an anaerobic storage duration of greater than eight months. Corn kernel moisture content averaged 24.6% (w.b.) at harvest and 30.6% when removed from storage. During the same storage period, stover moisture decreased from 48.0% at harvest to 43.8% (w.b.). At removal, kernel pH averaged 4.48, and the total fermentation acids were 1.65% of total grain dry matter (DM). The range of kernel moisture content was 26.5% to 34.7% (w.b.), which was much greater than when corn kernel physical properties were typically determined and reported [6–8].

The hypothesis of this research was that moist and fermented corn kernels will have different physical properties and flow characteristics than conventional dry corn kernels. These properties are needed for the design of equipment for post-storage handling and processing of these unique corn kernels. Therefore, the objective of this research was to quantify important physical properties and flow characteristics of corn kernels that have undergone prolonged storage with moist corn stover under anerobic conditions, where grain conservation occurred by fermentation.

2. Materials and Methods

2.1. Treatments, Material Preparation, and Parameters Quantified

Six treatments were considered: unfermented (U), conventional kernels at three different moistures (U–Low, U–Mid, U–High), two fermented (F) kernels at two different moistures (F–Low, F–High), and fermented kernels that had been oven dried (F–Dried). The U–Low and U–Mid kernels would be storage stable in typical grain storage structures. The U–High kernels could not be stored aerobically without concerns for biological deterioration. The different moistures of the unfermented and fermented treatments were achieved by harvesting at different dates (see below). The dried fermented treatment was created by oven drying fermented kernels at 65 °C until sufficient mass was removed so that the estimated moisture content was approximately 10% (w.b.). After oven drying, this treatment was allowed to equilibrate with the environment before tests were conducted. The grain hybrid was Dairyland DS-4018AMXT (Dairyland Seed Co., Kewaskum, WI,

USA) with a Comparative Relative Maturity of 101 days. This variety was a dent corn that typically has softer starch in the middle and top of the kernel compared to a flint corn that has hard starch throughout the kernel.

The F–Low and F–High material was co-stored with the stover fraction on 20 October and 5 November 2020, respectively. The material was packed in 60 L sealed plastic containers lined with 3 mil plastic bags. At storage, the contents were compressed with a hydraulic press to 140 kPa face pressure, and then the plastic bag was tightly sealed to maintain anerobic conditions. The containers were stored indoors at approximately 20 °C until removed from storage on 18 May 2021. Kernels were removed from the stover fraction by an air classification system. Quantification of physical properties began shortly after removal from storage, but separated kernels were stored in vacuum-sealed bags until tests began. The pH was 4.89 and 4.42, and the total fermentation acids were 0.78% and 1.94% of DM for the F–Low and F–High treatments, respectively. The F–Low and F–High treatments were tested at the moisture as removed from storage. There was no drying of these two treatments prior to testing.

All treatments had varying levels of foreign matter and broken grain; thus, a cleaning process was undertaken prior to testing. The grain was first fractionated in an ASABE particle-size separator [14]**.** The majority of whole kernels resided on the 6.4 mm screen, and this material was collected and then hand-cleaned to further remove additional broken kernels and foreign matter. After this process, the fermented treatments were stored in vacuum-sealed bags until tests were conducted. Unless specified otherwise, each treatment was replicated six times, and the replicate tests were conducted in a random order. At the time of testing, moisture content was determined by oven drying six random samples per treatment (each sample mass approximately 100 g) at 65 °C for 72 h [15].

A total of 18 different parameters were quantified to test the hypothesis that moist fermented corn kernels had different physical properties than typical dry grain (Table 1). These parameters are typical of those reported in the literature for dry corn kernels [6–13].

Table 1. Parameters quantified during experiments with moist fermented corn kernels and typical dry corn kernels.

Parameter Quantified	Symbol	Units	Parameter Quantified	Symbol	Units
Individual Kernels			Bulk Kernels		
Mass	m_k	g	Bulk Density [a]	ρ_b	$kg \cdot m^{-3}$
Length	d_1	mm	Friction Coefficient	μ	Unitless
Width	d_2	mm	Shear Stress	τ	kPa
Thickness	d_3	mm	Cohesion	C	kPa
Surface Area	SA	mm^2	Friction Angle	ϕ	degrees
Volume	V	mm^3	Rupture Force	F_r	N
Aspect Ratio	AR	Unitless	Breakage Susceptibility	BS	% of DM
Particle Density [a]	ρ_p	$kg \cdot m^{-3}$	Discharge Flow Rate [a]	$\dot{m}$	$kg \cdot s^{-1}$
			Angles of Repose [b]	ψ	degrees

[a]–Calculated on both a wet and dry matter basis. [b]–angles of repose determined three ways: anchor lifted (ψ_{al}); container discharge (ψ_{cd}); and hopper discharge (ψ_{hd}).

2.2. Dimensions and Surface Area

Length (d_1), width (d_2), thickness (d_3), and surface area (SA) of the kernels were quantified on 18 replicate intact kernels per treatment. Length, width, and thickness dimensions were quantified using a digital caliper with a 0.01 mm resolution. Aspect ratio (AR) was calculated from the ratio of width to length (d_2/d_1). To determine the surface area and volume of individual kernels, images of individual kernels were first taken with a Blackfly BFS-PGE-120S4C-CS camera (FLIR, Barrington, NJ, USA) equipped with a SL410M lens (Theia Technologies, Wilsonville, OR, USA). Images were analyzed using Matlab (ver. 2021a, MathWorks, Natick, MA, USA) by converting them into binary. A circular object of

a known surface area was used to calibrate the program. The count of white pixels in the binary image, which represented the kernel, was summed and used to calculate the surface area. Kernel volume (V) was estimated by multiplying the image surface area by the manually measured kernel thickness ($SA \cdot d_3$).

2.3. Particle and Bulk Density

Kernel particle density (ρ_p) was quantified using a water displacement method [16]. Replicate samples consisting of 30 kernels were weighed on a digital scale with 0.001 g resolution. Care was taken to randomly choose intact kernels that showed no visual evidence of breakage or splitting. Graduated cylinders were filled with 50 mL of room temperature distilled water, then 30 kernels per treatment were placed in the cylinder two kernels at a time. The final volume of the water and kernels was determined to the nearest 0.5 mL. Wet basis and dry basis particle densities were calculated using the volume of water displaced, number of kernels (30), mass of grain, and the moisture content of the treatment.

Kernel bulk density (ρ_b) was determined using a USDA standard [17] test weight apparatus (Model 29, Seedburo Equipment Co., Des Plaines, IL, USA). Enough grain was poured into the funnel to ensure the test container (473 mL) would overfill (Figure 1). The gate at the bottom of the funnel was removed, allowing grain to discharge into the container. The contents of the container were leveled using a gentle back-and-forth motion of a straight edge. The container and its contents were weighed to the nearest 0.01 g. Wet basis and dry basis bulk density were calculated using the container volume, mass of grain, and the moisture content of the treatment.

Figure 1. Grain emptying into container from discharge funnel (**left**). Leveling the contents with straight edge per USDA standard instructions [17] (**right**).

2.4. Friction with Various Surfaces

Kernel friction coefficient (μ) with four surfaces was determined using an adjustable tilting angle plate (part number 00675348, MSC Industrial, Melville, NY, USA) with a 13 × 18 cm surface. Four surface materials were used: ultra-high molecular weight polyethylene (UHMWPE), mild steel, stainless steel, and dry-graphite-coated mild steel. Each replicate sample consisted of approximately 60 g of kernels poured into a 65 mm diameter bottomless container (14.7 g mass). The container and contents were placed on the center of the back edge of the selected horizontal surface, and the container was lifted slightly so that only the grain was in contact with the surface (Figure 2). The table was slowly tilted until the container and its contents slid at least 5 cm down the surface. The angular displacement was halted, and the table slope was measured with a digital inclinometer (model 360, Kell-Strom Tool Co. Wethersfield, CT, USA) to the nearest 0.1 degree. The friction coefficient was calculated from the inverse tangent of the table slope.

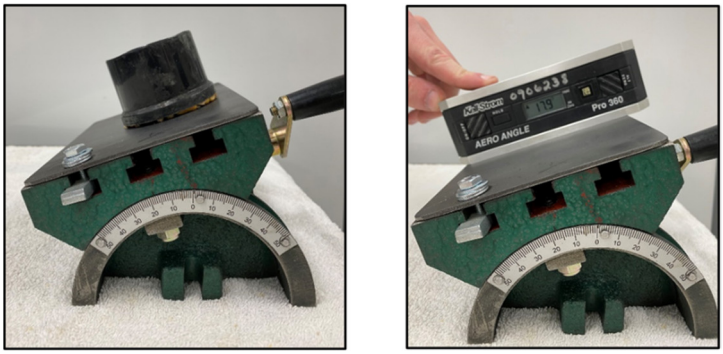

Figure 2. Apparatus used to measure friction coefficient. Note that the container was lifted, thus only kernels were in contact with the surface (**left**). The friction coefficient was estimated at the slope angle at which the kernel layer began to slide by overcoming the sliding friction resistance (**right**).

2.5. Direct Shear Test

A direct shear test was conducted at three normal stress levels to determine the apparent cohesion (C) and the angle of internal friction (ϕ) of corn kernels. The direct shear split cell was 100 × 100 mm, and each half of the cell was 25 mm deep. The lower cell was fixed, and the upper cell was pulled by a cable connected to an MTS Insight Standard Length universal testing machine (Edan Prairie, MN, USA) equipped with a 500 N rated load transducer (Figure 3). The upper and lower cells were separated by four UHMWPE pads, which provided a gap of approximately 1 mm, allowing for shearing between the kernels in the upper and lower cells. With the two cells in position, kernels were placed in the cell cavity, a square platen placed on the kernels, and a static load applied to the platen to produce three normal stress levels of 7, 14, and 21 kPa on the 100 × 100 mm shear cell area. The direct shear rate was 1 mm·s^{-1}. The horizontal force and horizontal displacement during shearing were recorded at 100 Hz. Over an approximate 15 mm total horizontal displacement, the shear stress and horizontal strain data exhibited shear strength measurement of the corn kernels.

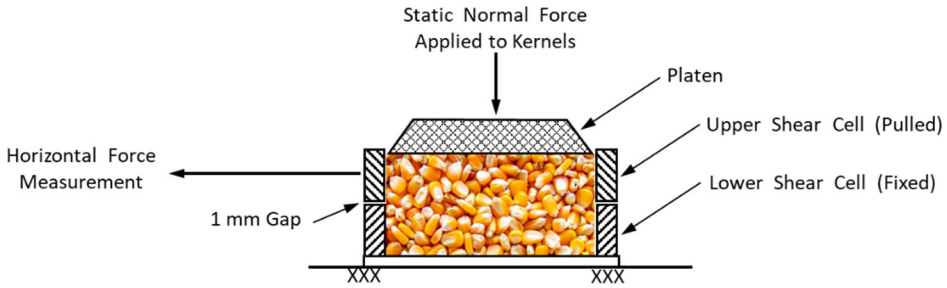

Figure 3. Schematic of shear test apparatus (not to scale). Cells were 100 mm square, each with 25 mm depth. Gap was created by four low-friction plastic pads.

Shear stress (τ) was calculated from the ratio of the shear force to the contact area between the lower and upper shear chambers. The contact area was calculated from the original cell dimensions and the recorded upper cell displacement. Kernel-to-kernel friction coefficient was calculated in two ways: μ_f was the ratio of maximum shear force to the applied normal force, and μ_s was the ratio of maximum shear stress to applied normal stress.

Using linear regression, the cohesive shear stress intercept and angle of internal friction were determined from the maximum shear stress for each normal stress levels and the normal stress applied during shearing for establishing the Mohr–Coulomb relationships, according to Equation (1):

$$\tau = C + \sigma \cdot \tan(\phi) \quad (1)$$

where τ is the shear stress, C is the apparent cohesion, σ is the normal stress, and ϕ is the kernel's angle of internal friction.

2.6. Kernel Rupture Strength

Kernel rupture strength (F_r) was determined using the MTS Insight Standard Length universal testing machine equipped with a 500 N rated load transducer. Eighteen kernels from each of the six treatments were selected at random, and the dimensions, masses, and surface areas were determined as described above (Section 2.2). Once the physical properties of each kernel were collected, kernels were randomly assigned to one of three orientations for compression testing (Figure 4). The compression machine was configured with flat plates, and the crosshead vertical loading speed was 3 mm·min^{-1}. The upper crosshead would lower onto the kernel while compression force (N), loading displacement (mm), and time (s) were recorded at 10 Hz until a rupture point was detected. Rupture force was defined as the force required to produce a compressive incipient break of the kernel specimen.

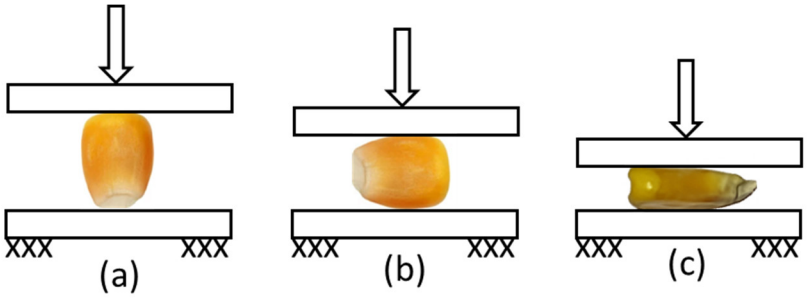

Figure 4. Orientations of kernels placed in compression force test machine (not to scale). The three selected orientations refer to the loading plane (**a**) perpendicular to the kernel major axis (vertical); (**b**) parallel to the kernel intermediate axis (side); and (**c**) parallel to kernel minor axis (flat).

2.7. Kernel Breakage Susceptibility

Breakage susceptibility (BS) was determined using the Wisconsin Breakage Tester (WBT), which employed an impeller that accelerated kernels toward a cylindrical steel impact surface. Details of the WBT can be found in [18]. To create kernel samples free of broken grain and foreign matter, each kernel treatment was screened through a 6.34 mm round hole sieve, and then further hand sorting was performed to remove any remaining broken or chipped kernels. The oven dry moisture content was used to determine the wet mass needed to create 150 g DM samples for each treatment. Each sample was individually fed into the WBT so that the entire mass was delivered to the WBT within 15 s. Samples were processed in random order. Each processed sample was sieved through a 4.75 mm round hole sieve. Material passing through the sieve was classified as fines. Material remaining on the sieve was hand sorted into whole and broken kernel fractions. All three fractions (fines, whole, and broken) were then oven dried at 105 °C for 24 h, and the amount in each of the three categories, expressed as a percentage of the total dry mass, was calculated.

2.8. Hopper Discharge Flow Rate

Hopper-discharged mass flow rate ($\dot{m}$) was determined using a polycarbonate cubic container with a 60-degree funnel at the bottom [7]. Three hopper discharge orifices were available: 100 × 100, 100 × 75, and 100 × 50 mm. The hopper opening was 100 × 100 mm; thus, the latter two orifices created rectangular annuluses with equal size flat overhangs of 12.5 and 25 mm, respectively, on two sides. The hopper was placed above an Ohaus

(Parsippany, NJ, USA) model Defender 5000 digital scale connected to a computer through an RS232 port. Data were acquired at 10 Hz with a resolution of 0.01 kg during the hopper grain discharging. A serial monitoring program was started, and the hopper discharge door was quickly opened, allowing material to flow onto a container on the scale until the hopper emptied. The first and last 1 s of transient data were removed to obtain the steady-state mass flow characteristics from the hopper experiment. A linear regression line was then fitted to the time versus measured mass to estimate the steady-state mass flow rate.

2.9. Angles of Repose

Anchor-lifted angles of repose (ψ_{al}) were determined using a method suggested by [16]. The device consisted of an acrylic cylinder with an inner diameter of 203 mm and a height of 185 mm (Figure 5). The anchor included a 15.7 mm diameter rod attached to a round flat bottom of 145 mm diameter with a 90 degree outside annular ring with a height of 13.5 mm.

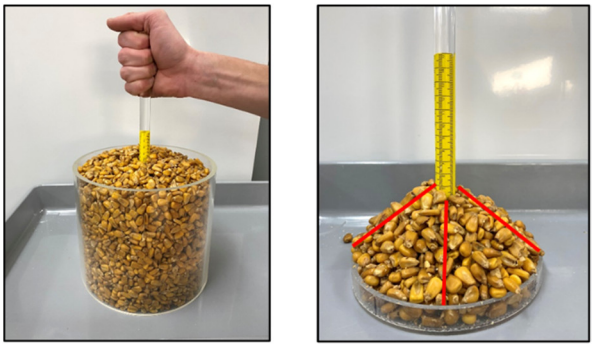

Figure 5. Anchor-lifted device filled with grain and the anchor being slowly lifted (**left**) to avoid particles agitation. Angle of repose was determined by measuring the pile height from the top of the anchor's annular ring to the top of the pile at four radial locations 90 degrees apart (**right**).

The anchor was placed in the center of the cylinder on a flat surface and grain added until its height was approximately 150 mm above the anchor base. The anchor was then lifted by hand until it was fully out of the cylinder. The height of the pile above the top of the annular ring was measured at four radial locations, 90 degrees apart around the circumference of the anchor cylinder (Figure 5). The slope to estimate the angles of repose was calculated from the arc tangent of the average pile height and the annular dimensions of the base.

Container discharge angles of repose (ψ_{cd}) were determined using a method suggested in [16]. The device consisted of an acrylic rectangular container (200 mm height, 250 mm length, and 120 mm depth) with a gate that formed one wall. The container was filled until level with the top, and then the gate was quickly lifted, allowing the material to discharge (Figure 6). A sheet of acrylic was gently placed on top of the sloped grain, and a digital inclinometer (Section 2.4) was used to measure the slope of the pile to the nearest 0.1 degree (Figure 6).

Figure 6. Grain filled discharge container (**left**). Measuring the angles of repose for discharged grain after the gate has been removed (**right**).

Hopper-discharged (ψ_{hd}) angles of repose were quantified using the mass flow rate hopper described above (Section 2.8). The hopper orifice was 100 × 100 mm. The hopper was placed with the orifice 45 cm above the ground, and the hopper was filled with approximately 22 L of grain. The hopper door was quickly opened, and the contents freely discharged. The slope of the resulting pile was quantified in four radial locations equidistant from each other around the circumference of the pile using the same digital inclinometer technique described above.

2.10. Statistical Analysis

Statistical analysis was completed using the Standard Least Squares method in the Fit Model platform of JMP Pro (ver. 15, SAS Institute Inc., Cary, NC, USA). All the differences among treatment means were compared using the Adjusted Tukey test, with significant differences declared at $p \leq 0.05$.

3. Results

3.1. Kernel Moisture Content and Mass

Each treatment had a statistically different moisture content, and fermented kernels had greater moisture than all other treatments (Table 2). Greater moisture content resulted in greater wet basis mass for individual kernels, but, when considered on a dry basis, there was no statistical difference in average kernel mass across all treatments.

Table 2. Moisture content and mass of individual kernels (m_k) (average, $n = 6$ for moisture content; and $n = 18$ for kernel mass).

Kernel Treatments		Moisture Content (MC) (% w.b.)	Kernel Mass (m)	
			Wet (g)	Dry (g)
Unfermented (U)				
	U–Low	8.5 f	0.323 e	0.295
	U–Mid	14.6 d	0.383 cd	0.327
	U–High	23.3 c	0.401 c	0.307
Fermented (F)				
	F–Low	26.1 b	0.445 b	0.328
	F–High	36.2 a	0.505 a	0.321
	F–Dried	9.9 e	0.358d e	0.323
SEM [a]		0.17	0.0106	0.0085
p-value [a]		<0.001	<0.001	0.478
LSD [a]		0.1	0.042	0.034

[a] Standard error of the mean. Within each column, lowercase markers indicate significant differences at $p < 0.05$ using Tukey's comparisons. Least square difference (LSD) for $p = 0.05$.

3.2. Kernel Dimensions

When placed into anerobic storage, the fermented kernels had similar moisture contents to the U–Mid kernels. The fermented kernels became larger during the prolonged anerobic storage period (Table 3). During storage, the width and thickness dimensions of the fermented kernels increased greater than the change in the length. During storage, the length increased by 1% while the width and thickness increased by 10% and 15%, respectively. The fermented kernels had a greater width, thickness, surface area, and volume than the drier kernels (U–Low, U–Mid, and F–Dried). There was no significant difference ($p < 0.05$) in kernel dimensions between the two fermented treatments (F–Low and F–High). The volume of the F–Low and F–High kernels was 26% and 30% greater, respectively, than the U–Mid kernels. The fermented and then dried kernels had similar dimensions, surface areas, and volumes to the U–Low and U–Mid unfermented kernels. The aspect ratio was greater for the fermented kernels than the unfermented U–Mid kernels.

Table 3. Dimensions, surface area, volume, and aspect ratio of individual corn kernels (average, n = 18).

Kernel Treatments [a]		Dimensions (mm)			Surface Area (SA)	Volume (V)	Aspect
		Length (d_1)	Width (d_2)	Thickness (d_3)	(mm^2)	(mm^3)	Ratio (AR)
Unfermented (U)							
	U–Low	13.40 bc	8.42 c	4.25 c	97 c	412 c	0.63 c
	U–Mid	13.49 bc	8.70 c	4.57 bc	98b c	448 bc	0.65 bc
	U–High	14.11a	8.82b c	4.49 c	111 a	497 b	0.63 c
Fermented (F)							
	F–Low	13.62 ab	9.41 ab	5.20 a	106 ab	563 a	0.70 a
	F–High	13.68 ab	9.62 a	5.32 a	112 a	581 a	0.70 a
	F–Dried	12.94c	8.97 bc	5.02 ab	90 c	443 bc	0.69 ab
SEM [b]		0.143	0.146	0.110	2.1	13.5	0.013
p-value [b]		<0.001	<0.001	<0.001	<0.001	<0.001	<0.001
LSD [b]		0.58	0.58	0.44	8	54	0.05

[a] Moisture content of the six treatments is found in Table 1. [b] Standard error of the mean. Within each column, lowercase markers indicate significant differences at $p < 0.05$ using Tukey's comparisons. Least square difference (LSD) for $p = 0.05$.

3.3. Particle and Bulk Density

The dry basis particle density was significantly less for the moist, fermented kernels compared to all other kernel treatments (Table 4). Drying these kernels significantly increased their dry basis particle density so that particle density of the F–Dried and U–Low kernels were similar. The U–High and F–Low kernels were both at approximately mid-20% moisture (Table 1) and had similar wet and dry basis particle density (Table 3). The fermented kernels had significantly lower dry basis bulk density than unfermented kernels with less than 15% moisture (i.e., U–Low and U–Mid). Across all treatments, both dry basis particle and bulk density decreased linearly ($r^2 = 0.82$) with moisture content.

Table 4. Wet and dry basis particle density of individual kernels and kernel bulk density (average, n = 6).

Kernel Treatments [a]	Particle Density (ρ_p) ($kg \cdot m^{-3}$)		Bulk Density (ρ_b) ($kg \cdot m^{-3}$)	
	Wet Basis	Dry Basis	Wet Basis	Dry Basis
Unfermented (U)				
U–Low	1181 ab	1081 a	733 a	671 a
U–Mid	1073 b	916 b	722 a	617 b
U–High	1108 b	849 bc	610 f	467 cd

Fermented (F)					
	F–Low	1171 ab	863 bc	642 e	488 c
	F–High	1276 a	796 c	699 c	437 d
	F–Dried	1131 b	1030 a	653 d	594 b
SEM [b]		26.8	22.8	2.2	7.5
p-value [b]		<0.001	<0.001	<0.001	<0.001
LSD [b]		108	94	8	32

[a] Moisture content of the six treatments is found in Table 1. [b] Standard error of the mean. Within each column, lowercase markers indicate significant differences at $p < 0.05$ using Tukey's comparisons. Least square difference (LSD) for $p = 0.05$.

3.4. Kernel Friction Coefficient on Various Surfaces

Compared to the U–Low and U–Mid kernels, the fermented kernels had a greater friction coefficient on all four surfaces (Table 5). The F–High kernels had a greater friction coefficient than the F–Low kernels on three of the surfaces tested. For most surfaces, the U–High kernels had a similar friction coefficient to the F–Low and F–High kernels. Across all treatments, the friction coefficients were less for the UHMWPE and graphite-coated steel than the other two surfaces. There was no statistical difference in the friction coefficient between the U–Low and F–Dried kernels on the three steel surfaces.

Table 5. Friction coefficient of corn kernels to four different surfaces (average, $n = 6$).

Kernel Treatments [a]	**Friction Coefficient (μ)**			
	UHMWPE [b]	**Steel**		
		Mild	**Stainless**	**Dry Graphite Coated**
Unfermented (U)				
U–Low	0.29 c	0.31 c	0.32 c	0.25 c
U–Mid	0.23 d	0.40 b	0.37 c	0.24 c
U–High	0.38 a	0.49 a	0.52 ab	0.44 ab
Fermented (F)				
F–Low	0.33 b	0.45 ab	0.48 b	0.43 b
F–High	0.37 a	0.49 a	0.53 a	0.46 a
F–Dried	0.22 d	0.29 c	0.33 c	0.24 c
SEM [c]	0.007	0.014	0.012	0.008
p-value [c]	<0.001	<0.001	<0.001	<0.001
LSD [c]	0.03	0.06	0.05	0.03

[a] Moisture content of the six treatments is found in Table 1. [b] Ultra-high molecular weight polyethylene. [c] Standard error of the mean. Within each column, lowercase markers indicate significant differences at $p < 0.05$ using Tukey's comparisons. Least square difference (LSD) for $p = 0.05$.

3.5. Shear Strength Properties of Kernels

The fermented (F) kernels had a greater angle of internal friction than the unfermented (U) kernels (Table 6, Figure 7). The low moisture unfermented kernels (U–Dry) had the numerically smallest friction angle and the lowest cohesion. Drying the fermented kernels (F–Dried) reduced the friction angle and cohesion. In almost all cases, the kernel-to-kernel friction coefficient was greater for the fermented kernels than unfermented kernels (Table 7). Independent of kernel treatments, the kernel-to-kernel friction coefficient decreased with a greater normal pressure.

Table 6. Kernel's shear strength parameters of apparent cohesion (C) and angle of internal friction (ϕ) (average, $n = 6$).

Parameter [a]	Unfermented (U) Kernels [b]			Fermented (F) Kernels [b]		
	U–Low	U–Mid	U–High	F–Low	F–High	F–Dried
Cohesion: C (kPa)	0.51	1.68	1.26	2.49	2.14	0.79
Angle of internal friction: ϕ (deg)	27.3	29.6	29.2	35.0	36.1	30.1
r^2	0.9984	0.9977	0.9999	0.9980	0.9999	0.9963

[a] Coefficients for Mohr–Coulomb equation–see Equation (1). [b] Moisture content of the six treatments is found in Table 1.

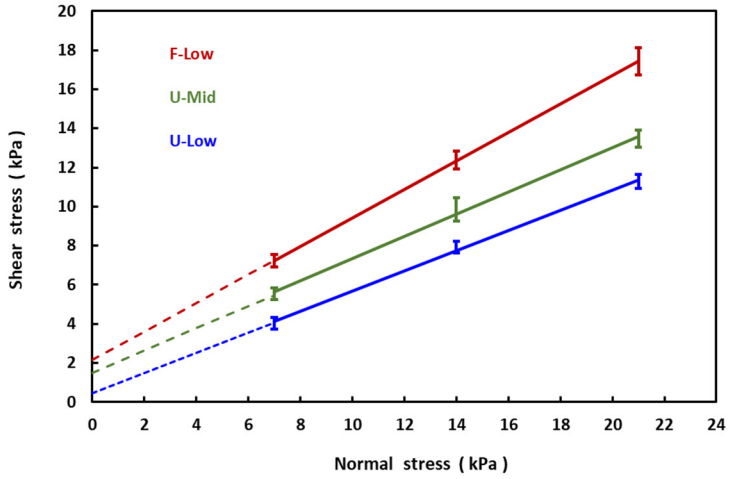

Figure 7. Normal stress versus maximum shear stress for the direct shear testing. Treatments are unfermented kernels with two moisture contents (U–Low and U–Mid, 8.5% and 14.6% (w.b.), respectively) and fermented kernels (F–Low, 26.1% (w.b.)). Error bars represent the standard error of the mean ($n = 6$).

Table 7. Kernel-to-kernel friction coefficients estimated from the direct shear tests (average, $n = 6$).

Kernel Treatments [a]	Ratio of Normal and Maximum Shear Forces (μ_f)			Ratio of Normal and Maximum Shear Stresses (μ_s)		
	Normal Stress Levels					
	7 kPa	14 kPa	21 kPa	7 kPa	14 kPa	21 kPa
Unfermented (U)						
U–Low	0.52 c	0.50 c	0.46 c	0.57 c	0.57 b	0.51 c
U–Mid	0.69 b	0.63 b	0.57 ab	0.79 b	0.70 b	0.64 b
U–High	0.64 bc	0.57 bc	0.53 b	0.74 bc	0.65 b	0.62 bc
Fermented (F)						
F–Low	0.91 a	0.83 a	0.70 a	1.06 a	0.96 a	0.81 a
F–High	0.88 a	0.79 a	0.67 ab	1.03 a	0.93 a	0.80 a
F–Dried	0.64 bc	0.56 bc	0.56 ab	0.71 bc	0.62 b	0.62 bc
SEM [b]	0.033	0.027	0.023	0.041	0.034	0.02
p-value [b]	<0.001	<0.001	<0.001	<0.001	<0.001	<0.001
LSD [b]	0.13	0.11	0.16	0.17	0.13	0.12
Averaged independent of treatment [c]	0.71a	0.65b	0.58c	0.82a	0.74b	0.67c

[a] Moisture content of the six treatments is found in Table 1. [b] Standard error of the mean. Within each column, lowercase markers indicate significant differences at $p < 0.05$ using Tukey's comparisons. Least square difference (LSD) for $p = 0.05$. [c] The SEM, *p*-value, and LSD were 0.012, <0.001, and 0.10; and 0.015, <0.001, and 0.12, for μ_f and μ_s, respectively.

3.6. Kernel Rupture Force

Less force was required to rupture kernels in the side and vertical orientation than when laid flat because the force was distributed over a greater surface area in the flat orientation (Table 8). The fermented kernels (F–Low and F–High) required less force to rupture than the unfermented kernels with less than 15% moisture content (U–Low and U–Mid). After drying, the fermented kernels (F–Dried) also required less force to rupture than the unfermented kernels with less than 15% moisture content (U–Low and U–Mid). There were no statistical differences in rupture forces between the U–High kernels and the two fermented kernels (F–Low and F–High).

Table 8. Rupture force (F_r) of individual kernels configured in three different orientations (average, $n = 6$).

Kernel Treatments [a]		Rupture Force (N)		
		Kernel Orientation [b]		
		Side	**Vertical**	**Flat**
Unfermented (U)				
	U–Low	178 a	153 ab	331 a
	U–Mid	137 b	165 a	320 ab
	U–High	72c	66 c	274 ab
Fermented (F)				
	F–Low	80 c	62 c	281 ab
	F–High	73 d	66 c	250 ab
	F–Dried	84 c	99 bc	191 b
SEM [c]		9.4	13.2	26.8
p-value [c]		<0.001	<0.001	0.012
LSD [c]		40	54	109

[a] Moisture content of the six treatments is found in Table 1. [b] Kernel orientation in the test fixture, see Figure 4. [c] Standard error of the mean. Within each column, lowercase markers indicate significant differences at $p < 0.05$ using Tukey's comparisons. Least square difference (LSD) for $p = 0.05$.

3.7. Breakage Susceptibility

The U–High and F–Low kernels were the least prone to damage in the centrifugal breakage test (Table 9). There was a tendency for greater damage as moisture content of the fermented kernels increased (F–High vs. F–Low). Drier unfermented kernels (U–Low and U–Mid) had greater damage than moist unfermented kernels (U–High). The fermented and dried kernels (F–Dried) were the most susceptible to damage with, by far and away, the most fines of any treatments.

Table 9. Breakage susceptibility (BS) of kernel treatments after being subjected to centrifugal breakage test (average, $n = 6$).

Kernel Treatments [a]		Fraction of Total DM (%)		
		Whole	**Broken**	**Fines**
Unfermented (U)				
	U–Low	28.6 cd	59.9 a	11.4 b
	U–Mid	38.7 cd	56.7 a	4.6 cd
	U–High	85.5 a	14.1 b	0.4 d
Fermented (F)				
	F–Low	78.4 ab	20.1 b	1.6 cd
	F–High	54.7 bc	37.7 ab	7.6 bc
	F–Dried	10.7 d	56.1 ab	33.1 a
SEM [b]		6.78	6.64	1.51
p-value [b]		<0.001	<0.001	<0.001

LSD [b]	28.4	28.1	6.2

[a] Moisture content of the six treatments is found in Table 1. [b] Standard error of the mean. Within each column, lowercase markers indicate significant differences at $p < 0.05$ using Tukey's comparisons. Least square difference (LSD) for $p = 0.05$.

3.8. Discharge Flow Rate

The discharge flow rate decreased for all treatments as the orifice size became smaller (Table 10). For all three orifice sizes, the unfermented grain (U–Mid) and fermented and dried (F–Dried), they had the greatest dry basis steady-state flow rates. Compared to the U–Mid treatment, the dry basis flow rate was 25%, 26%, and 27% less (F–Low) and 31%, 33%, and 35% less (F–High) for the 100 × 100, 75 × 100, and 50 × 100 mm orifices, respectively. For each orifice size and all treatments, the dry basis flow rate decreased linearly with increasing moisture content ($r^2 = 0.83$ to 0.89). Across all treatments, the dry basis flow rate decreased by approximately 33% as the orifice size decreased from 100 × 100 mm to 75 × 100 mm and by approximately 50% as the orifice size decreased from 75 × 100 mm to 50 × 100 mm.

Table 10. Wet and dry basis container discharge flow rate ($\dot{m}$) from three orifice sizes (average, $n = 6$).

Kernel Treatments [a]	**Mass Flow Rate (kg·s^{-1})**					
	Orifice Dimensions (mm)					
	100 × 100		**75 × 100**		**50 × 100**	
	Wet Basis	**Dry Basis**	**Wet Basis**	**Dry Basis**	**Wet Basis**	**Dry Basis**
Unfermented (U)						
U–Mid	3.61 a	3.09 a	2.44 a	2.09 a	1.24 a	1.06 a
Fermented (F)						
F–Low	3.16 c	2.31 b	2.10 c	1.54 c	1.06 c	0.77 c
F–High	3.40 b	2.12 c	2.23 b	1.40 d	1.13 b	0.70 d
F–Dried	3.39 b	3.08 a	2.10 c	2.02 b	1.02 d	0.99 b
SEM [b]	0.033	0.029	0.015	0.011	0.001	0.006
p-value [b]	<0.001	<0.001	<0.001	<0.001	<0.001	<0.001
LSD [b]	0.14	0.12	0.06	0.07	0.02	0.02

[a] Moisture content of the six treatments is found in Table 1. There was insufficient material to conduct this experiment with the U–Low and U–High kernel treatments. [b] Standard error of the mean. Within each column, lowercase markers indicate significant differences at $p < 0.05$ using Tukey's comparisons. Least square difference (LSD) for $p = 0.05$.

3.9. Angles of Repose

The angles of repose were determined using three different methods: container discharge, anchor lifted, and hopper discharge (Table 11). The fermented kernels (F–Low and F–High) had greater angles of repose than the unfermented U–Low and U–Mid kernels using all three methods. For container discharge and anchor lift methods, the high moisture unfermented grain (U–High) had similar or greater angles of repose than the F–Low and F–High kernels. Dried fermented kernels (F–Dried) had smaller angles of repose than the two fermented kernel treatments (F–Low and F–High).

Table 11. Angles of repose (ψ) as determined by three different methods (average, $n = 6$).

Kernel Treatments [a]		Angles of Repose (deg)		
		Container Discharge (ψ_{cd})	Anchor Lifted (ψ_{al})	Hopper Discharge [b] (ψ_{hd})
Unfermented (U)				
	U–Low	19.0 c	27.6 d	
	U–Mid	18.5 c	26.2 d	20.0 c
	U–High	32.5 a	41.0 a	
Fermented (F)				
	F–Low	31.5 a	37.4 b	31.0 a
	F–High	32.3 a	38.6 b	32.0 a
	F–Dried	22.8 b	30.3 c	25.4 b
SEM [c]		0.32	0.36	0.29
p-value [c]		<0.001	<0.001	<0.001
LSD [c]		1.4	1.2	1.4

[a] Moisture content of the six treatments is found in Table 1. [b] There was insufficient quantity of material to conduct this experiment with the U–Low and U–High kernel treatments. [c] Standard error of the mean. Within each column, lowercase markers indicate significant differences at $p < 0.05$ using Tukey's comparisons. Least square difference (LSD) for $p = 0.05$.

4. Discussion

Dry corn kernels gained moisture and were conserved by fermentation during prolonged anaerobic storage with corn stover at 40% to 55% w.b. moisture content. These kernels exhibited different physical properties than unfermented kernels at typical storage moisture (i.e., less than 15% w.b.). The fermented kernels increased in size during storage, noticeably increasing in width, thickness, surface area, and volume (Table 3). Barnwell et al. [13] reported that kernel diameter, surface area, and volume increased as the moisture content of unfermented kernels increased from 13% to 29% (w.b.), and kernel dimensions increased linearly as moisture content increased. Kernel dimensions, surface area, and volume were also found to increase with moisture content [6,8].

It is envisioned that at removal from anaerobic storage, the comingled grain and stover will be quickly transported to a biorefinery where separation of these two fractions will occur soon after delivery. It is unlikely that fermented corn kernels separated from stover will have a long storage duration before end use because the fermentation level is low and aerobic heating could be an issue [4]. For this reason, it is also unlikely that kernels will be stored in large grain bins, where packing from pressure of large overlaying grain mass will affect bulk density. Nonetheless, short term storage will be required, and greater storage volume will be required for the fermented grain because of the low particles and bulk densities of the fermented treatments (Table 4). A similar decrease in wet basis bulk density with a greater moisture of unfermented kernels was reported in [6,8,13]. The fermented kernels had smaller dry basis bulk density due to larger kernel volume (Table 3) and greater kernel to kernel friction (Table 7), which impacted flow into the standard density cup.

Friction coefficient is an important grain physical parameter in the design of material handling and storage devices. For instance, friction coefficient is required to determine the allowable inclination angle for belt conveying [19], to estimate the capacity and power requirements of screw conveyors [20], and to determine the critical bin angles that provide consistent flow at unloading [21]. In all cases, fermented kernels had greater friction coefficients than unfermented kernels with less than 15% (w.b.) moisture content. This was true for kernel sliding on various surfaces (Table 4) and kernel-to-kernel friction (Table 7). However, friction coefficients were not statistically different between the U–High and F–Low kernels at similar moisture contents. Whether the kernels were fermented or

unfermented, greater moisture content may result in increased adhesion characteristics and surface roughness, increasing their friction characteristics. Similar to the results reported here, corn kernel friction coefficients on various surfaces increased linearly with moisture content [8].

Looking at the shear strength parameters, the internal friction angles reported here were similar to those reported in [7], but the cohesions were much less (Table 6). The disparities in the apparent cohesion of kernels reported in [7] and the data in Table 5 appeared to be influenced by the differences in normal stress. The normal stress levels used for estimating the kernel apparent cohesion in [7] (range 94 to 265 kPa) were greater than the normal stress levels (7 to 21 kPa) applied for measuring the cohesion of fermented and unfermented kernels in this study. The angle of internal friction and apparent cohesion were greater for the fermented kernels than the unfermented kernels, even when the moisture contents were similar (i.e., U–High vs. F–Low, Table 6). The increase in shear strength parameters of the internal friction angles and cohesion at greater moisture content was likely due to greater moisture near the kernel surface causing stickiness (cohesion) between the interacting kernels. The moisture content-dependent Mohr–Coulomb shear strength values allowed for an accurate estimate of the maximum shear forces required for designing the transport or discharge of moist kernels (fermented or unfermented) in unconsolidated or consolidated stress states.

Rupture force was defined as the force required to produce a major break in the kernel. Previous research has shown that unfermented kernels had lower rupture force as kernel moisture content increased [7,8,13,22]. Rupture force was statistically less for the F–Low and F–High fermented kernels than for the U–Low and U–Mid kernels (Table 8). Low rupture force could lead to greater kernel damage during handling, creating excessive fines that reduce conveyance efficiency or collect in undesirable locations. However, the F–Low and F–High kernels exhibited less tendencies for breakages than the U–Low and U–Mid kernels (Table 9). Breakages of unfermented kernels decreased in centrifugal breakage tests as moisture content increased [23], similar to results here. The fermented and then dried kernels (F–Dried) were particularly prone to breakage and produced the greatest fractions as fines. The low rupture forces of the fermented kernels could be considered an attribute if the power required for size reduction in hammer or roller mills is reduced.

The flow characteristics measured from the angles of repose are an important property of bulk grain that describes the inter-particle frictional resistance and unconsolidated flow behavior. The bulk angle of response is affected by a combination of many factors, including particle-to-particle sliding and rolling frictional forces interacting as the pile is formed, particle shape and size, and kernel moisture content [21]**.** Previous research has shown that the corn kernel angles of repose increased with the moisture content [6,8]. The greater moisture content of the fermented kernels increased friction forces between particles (Tables 6 and 7), increasing the frictional resistance to sliding and rolling, which resulted in greater angles of repose (Table 11). The anchor-lifted angles of repose were greater than the bucket-discharged angles of repose (Table 11). Similar results were reported for dry corn kernels [7]. In the latter method, the angles of repose were influenced by the effects of kernel-to-kernel and kernel-to-wall friction, whereas, in the former method, the angles of repose were impacted by sliding and rolling kernel-to-kernel friction. All three methods showed the angles of repose from the moist fermented kernels was greater than the data from the relatively drier unfermented kernels (Table 11). These testing methods could be used for in situ measurement of bulk flow behavior of kernels, fermented or unfermented, in biomass conveying or storage equipment.

Fermented kernels exhibited a lower dry basis discharge flow rate than unfermented U–Mid kernels (Table 10). The discharge flow rate was significantly less for the F–High kernels than the F–Low kernels (Table 10). Steady-state discharge flow rate decreased by 20% as the moisture content of unfermented kernels increased from 16% to 26% (w.b.) [7]. During hopper discharge, kernels slid over one another and on the container walls to flow

out of the hopper's orifice. The fermented kernels had greater surface-to-kernel and kernel-to-kernel friction coefficients and greater angles of repose than dry unfermented kernels (U–Mid), which contributed to the reduction in dry basis mass flow.

5. Conclusions

Fermented corn kernels at 26% to 35% (w.b.) moisture content exhibited different physical properties than typical dry unfermented kernels (i.e., less than 15% w.b.). The fermented kernels had larger dimensions, smaller particles and bulk densities, smaller rupture forces, greater friction coefficients and angles of repose, and lower container discharge flow rates. Based on these results, it is likely that fermented kernels stored in bulk will require greater storage volumes, may be more difficult to remove from storage bins, and require larger conveyance mechanisms to achieve similar flow rates as dry corn kernels.

Author Contributions: Conceptualization, K.J.B. and K.J.S.; methodology, K.J.B., K.J.S., and M.F.D.; formal analysis, K.J.B. and K.J.S.; investigation, K.J.B., Z.A.K., and K.J.S.; resources, K.J.S., M.Z.T. and Z.A.K.; writing—original draft preparation, K.J.B. and K.J.S.; writing—review and editing, K.J.B., K.J.S., M.Z.T. and M.F.D.; supervision, K.J.S. and M.F.D.; project administration, M.F.D. and K.J.S. All authors have read and agreed to the published version of the manuscript.

Funding: This research was supported by the U.S. Department of Energy (DOE), Office of Energy Efficiency and Renewable Energy (EERE), Bioenergy Technologies Office (BETO), under Award No. DE-EE0008908. The views expressed in this chapter do not necessarily represent the views of the U.S. Department of Energy or the United States Government.

Data Availability Statement: Raw data are not publicly available, although the data may be made available on request from the corresponding author.

Acknowledgments: This research could not have been completed without the assistance of the staff of the University of Wisconsin Arlington Agricultural Research Station.

Conflicts of Interest: The authors declare no conflicts of interest.

References

1. Wendt, L.M.; Smith, W.A.; Hartley, D.S.; Wendt, D.S.; Ross, J.A.; Sexton, D.M.; Lukas, J.C.; Nguyen, Q.A.; Murphy, J.A.; Kenney, K.L. Techno-economic assessment of a chopped feedstock logistics supply chain for corn stover. *Front. Energy Res.* **2018**, *6*, 90. https://doi.org/10.3389/fenrg.2018.00090.
2. Walters, C.P.; Dietsche, S.C.; Keene, J.R.; Friede, J.C.; Shinners, K.J. Increasing single-pass corn stover yield by combine header modifications. *Transact. ASABE* **2020**, *63*, 923–932. https://doi.org/10.13031/trans.13823.
3. Cook, D.E.; Shinners, K.J.; Weimer, P.J.; Muck, R.E. High dry matter whole-plant corn as a biomass feedstock. *Biomass Bioenergy* **2014**, *64*, 230–236. https://doi.org/10.1016/j.biombioe.2014.02.026.
4. Pike, B.C.; Shinners, K.J.; Timm, A.J.; Friede, J.C.; Digman, M.F. Co-harvest and anaerobic co-storage of corn grain and stover as biomass feedstocks. *J. ASABE* **2023**, *66*, 423–430. https://doi.org/10.13031/ja.15299.
5. Blazer, K.J. Anatomical Fractionation of Corn Grain and Stover to Produce Biomass Feedstocks. Master's Thesis, Department of Biological Systems Engineering, University of Wisconsin, Madison, WI, USA, 2022, Unpublished.
6. Bhise, S.; Kaur, A.; Manikantan, M. Moisture dependent physical properties of maize (PMH-1). *Acta Aliment.* **2014**, *43*, 394–401. https://doi.org/10.1556/aalim.43.2014.3.5.
7. Mousaviraad, M.; Tekeste, M.Z. Effect of grain moisture content on physical, mechanical, and bulk dynamic behaviour of maize. *Biosyst. Eng.* **2020**, *195*, 186–197. https://doi.org/10.1016/j.biosystemseng.2020.04.012.
8. Seifi, M.R.; Alimardani, R. The moisture content effect on some physical and mechanical properties of corn (Sc 704). *J. Agric. Sci.* **2010**, *2*, 125. https://doi.org/10.5539/jas.v2n4p125.
9. Tarighi, J.; Mahmoudi, A.; Alavi, N. Some mechanical and physical properties of corn seed (Var. DCC 370). *Afr. J. Agric. Res.* **2011**, *6*, 3691–3699.
10. Kruszelnicka, W.; Chen, Z.; Ambrose, K. Moisture-dependent physical-mechanical properties of maize, rice, and soybeans as related to handling and processing. *Materials* **2022**, *15*, 8729. https://doi.org/10.3390/ma15248729.
11. Wei, H.; Zan, L.; Li, Y.; Wang, Z.; Saxén, H.; Yu, Y. Numerical and experimental studies of corn particle properties on the forming of pile. *Powder Technol.* **2017**, *321*, 533–543. https://doi.org/10.1016/j.powtec.2017.08.051.
12. Sangamithra, A.; Gabriela, J.S.; Prema, R.S.; Nandini, K.; Kannan, K.; Sasikala, S.; Suganya, P. Moisture dependent physical properties of maize kernels. *Int. Food Res. J.* **2016**, *23*, 109–115.

13. Barnwal, P.; Kadam, D.M.; Singh, K.K. Influence of moisture content on physical properties of maize. *Int. Agrophys.* **2012**, *26*, 331–334. https://doi.org/10.2478/v10247-012-0046-2.
14. *Standard S424.1*; Method of Determining and Expressing Particle Size of Chopped Forage Materials by Screening. ASABE: St. Joseph, MI, USA, 2017.
15. *ASAE Standard 352.2*; Moisture Measurement—Unground Grain and Seed. ASABE: St. Joseph, MI, USA, 2017.
16. Tekeste, M.Z.; Mousaviraad, M.; Rosentrater, K.A. Discrete element model calibration using multi-responses and simulation of corn flow in a commercial grain auger. *Transact. ASABE* **2018**, *61*, 1743–1755. https://doi.org/10.13031/trans.12742.
17. USDA. Practical Inspection Procedures for Grain Handlers. 2016. Available online: https://www.ams.usda.gov/sites/default/files/media/PracticalProceduresBook2017.pdf (Accessed on April 26, 2023).
18. Singh, S.S.; Finner, M.F. A centrifugal impacter for damage susceptibility evaluation of shelled corn. *Transact. ASAE* **1983**, *26*, 1858–1863. https://doi.org/10.13031/2013.33856.
19. Hrabovský, L.; Fries, J. Transport performance of a steeply situated belt conveyor. *Energies* **2021**, *14*, 7984. https://doi.org/10.3390/en14237984.
20. Rademacher, F.J.C. On seed damage in grain augers. *J. Agric. Eng. Res.* **1981**, *26*, 87–96. https://doi.org/10.1016/0021-8634(81)90129-3.
21. Bhadra, R.; et al. Field-observed angles of repose for stored grain in the United States. *Appl. Eng. Agric.* **2017**, *33*, 131–137. https://doi.org/10.13031/aea.11894.
22. Mancera-Rico, A.; García-de-los-Santos, G.; Zavaleta-Mancera, H.A.; Carrillo-Salazar, J.A.; González-Estrada, E.; Villaseñor-Perea, C.A. Moisture and rupture models for corn (Zea mays) seeds of different endosperm types. *Transact. ASABE* **2019**, *62*, 913–918. https://doi.org/10.13031/trans.13021.
23. Eckhoff, S.R.; Wu, P.C.; Chung, D.S.; Converse, H.H. Moisture content and temperature effects on Wisconsin breakage tester results. *Transact. ASAE* **1988**, *31*, 1241–1246. https://doi.org/10.13031/2013.30851.